Cavity ringdown laser absorption spectroscopy and time-of-flight mass spectroscopy of jet-cooled gold silicides

J. J. Scherer,[a] J. B. Paul, C. P. Collier, A. O'Keefe,[b] and R. J. Saykally
Department of Chemistry, University of California, Berkeley, California 94720

(Received 8 May 1995; accepted 14 August 1995)

The cavity ringdown technique has been employed for the spectroscopic characterization of the AuSi molecule, which is generated in a pulsed supersonic laser vaporization plasma reactor. Fifteen rovibronic bands have been measured between 340 nm–390 nm, 8 of which have been analyzed to yield molecular properties for the X and $D\ ^2\Sigma$ states of AuSi. This assignment is in disagreement with previous emission studies of AuSi, which had assigned the ground electronic state as a $^2\Pi$ state. A time-of-flight mass spectrometer simultaneously monitors species produced in the molecular beam and has provided evidence for facile formation of polyatomic gold silicides. Comparison of AuSi with our recent results for CuSi and AgSi indicates regular bonding trends for the three coinage metal silicide diatoms. © *1995 American Institute of Physics.*

I. INTRODUCTION

As is the case for the other coinage metal silicides, current research on gold–silicides has focused primarily on their solid state properties. In particular, the electronic properties of gold–silicon compounds and interfaces have been studied,[1] including the measurement of Schottky diode barrier behavior in copper doped Au–Si films.[2] Evidence for the existence of metastable Au–Si structures at gold–silicon interfaces has also been obtained.[3] In one high resolution TEM study, spherical Au–Si nanoclusters were observed under certain annealing conditions.[4] Similar to copper silicides, electromigration of Au into Si lattices has been observed,[5] although the mechanisms responsible for this effect are not well understood. Detailed information on the formation of and bonding in Au–Si systems is accessible through gas phase spectroscopic studies of small molecular systems, and may contribute to our understanding of some of the above phenomena. However, to date, few gas phase studies of gold silicides have been performed.

The only gold silicide which has been studied in the gas phase is the AuSi diatom. The first published data for AuSi consist of a brief report on the vibronically resolved emission spectra for two near infrared band systems by Barrow *et al.*[6] in 1964. In this low resolution work, the emission spectra of AuSi produced in a high temperature King furnace were recorded in the 790 nm region, and assigned as belonging to a $^2\Sigma$–$X\ ^2\Pi$ system, based on the appearance of Q-branch heads. Because of spectral congestion, several of the observed bands could not be assigned, and were further complicated by the presence of both red and blue degraded bandheads. Nevertheless, a ground state vibrational frequency of 391 cm^{-1} was reported. Five years later, the ground state dissociation energy (3.308 eV) for the AuSi diatom was obtained in the Knudsen effusion mass spectrometric measurements of Gingerich.[7]

The emission bands studied by Barrow *et al.* were reinvestigated in 1973 by Houdart and Schamps,[8] who also proposed a $^2\Sigma$–$X\ ^2\Pi$ vibronic assignment. In this study, an additional band system was observed between 700–760 nm which possessed obvious vibronic progressions. Analysis of this system yielded vibrational frequencies for the ground and excited states of 390.9 and 389.5 cm^{-1}, respectively. These two band systems were assigned as $A\ ^2\Sigma$–$X\ ^2\Pi_{1/2}$ and $A\ ^2\Sigma$–$X\ ^2\Pi_{3/2}$, with an associated ground state spin–orbit splitting of 1071 cm^{-1}. This assignment appears questionable, since common upper state vibrational frequencies were not identified. The 750 nm system was reinvestigated later by Coquant and Houdart,[9] who again proposed a $^2\Sigma$–$X\ ^2\Pi$ assignment. A potential source of confusion in this report is the inconsistent nomenclature used in labeling of the states. Bands previously assigned as $A\ ^2\Sigma$–$X\ ^2\Pi_{1/2}$ are designated as B–X in the work of Coquant *et al.*, while those previously assigned as $A\ ^2\Sigma$–$X\ ^2\Pi_{3/2}$ remain assigned as A–X. In the discussions which follow, we will employ the standard X_1 and X_2 nomenclature for the proposed different spin–orbit manifolds and maintain the upper A state designation in this section for the sake of clarity. The rotational analysis of the 0-0 and 1-1 bands of the A–X_1 system presented in Ref. 9 yielded rotational constants (and associated bond lengths) of 0.0617 cm^{-1} (3.34 Å) and 0.0637 cm^{-1} (3.29 Å) for the A and X_1 states, respectively. The 790 nm A–X_2 system was not measured in that study. The CRLAS data for AuSi presented in this paper suggest that the previous rotational analysis and ground state symmetry assignment are incorrect.

II. EXPERIMENT

A. Cavity ringdown laser absorption spectroscopy (CRLAS)

The complete history and development of the cavity ringdown technique can be found in our recent review article.[10] In the pulsed cavity ringdown technique, first developed by O'Keefe and Deacon in 1987 for the determination of mirror reflectivities,[11] molecular absorption is deconvoluted from the measured photon decay time of a high

[a]Present address: Combustion Research Facility, Sandia National Laboratories, Livermore, California 94551.
[b]Los Gatos Research, 1685 Plymouth St., Mountain View, California 94043.

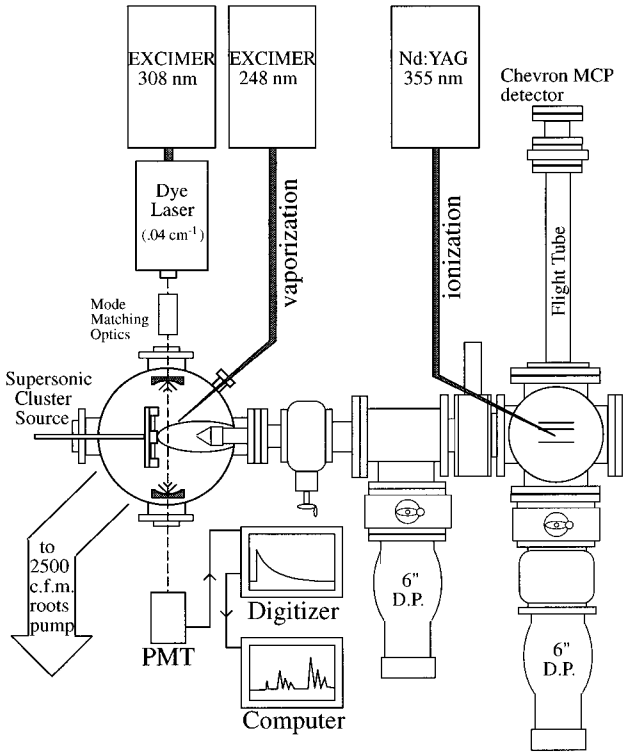

FIG. 1. Berkeley CRLAS/TOFMS apparatus. A laser vaporized pulsed molecular beam of supersonic metal silicide clusters is generated in a vacuum chamber and perpendicularly intersected by the ringdown laser. The ringdown decay is timed to coincide with the transient molecular beam and the fitted region of the decay is tailored for maximum absorption.

finesse optical cavity which is injected with a short pulse of laser light. The high sensitivity of this technique was first demonstrated by O'Keefe *et al.* by measuring doubly forbidden optical transitions in molecular oxygen.[11] Since our first application of the cavity ringdown technique to the study of pulsed molecular beams,[12] several other researchers have employed the technique for various purposes, including gas cell spectroscopy of HCN,[13,14] adaptation to kinetics studies,[15] the spectroscopy of OH in flames,[16] and the detection of CH_3 in a hot filament flow reactor.[17]

The Berkeley Cavity Ringdown Laser Absorption Spectrometer and time-of-flight mass spectrometer (TOFMS) are diagrammed in Fig. 1. The apparatus has been described in detail elsewhere[18,19] and will therefore only be briefly outlined here. The design consists of a main source chamber evacuated by a large Roots pump (2500 cfm Edwards EH4200), and two diffusion pumped regions, each separated by 2 mm skimmers. The tandem design of the apparatus allows characterization of the molecular beam while simultaneously monitoring absorption features, which greatly aids in the maximization of cluster concentrations and also allows correlation studies to be performed.

The 15 ns ringdown laser pulse consists of 1–2 mJ of narrowband (0.04 cm^{-1}) excimer-pumped dye laser light which is coupled into the cavity with the use of a telescope. Roughly 1 part in 10^8 of the incident light passes through the exit mirror of the cavity and is detected with a photomultiplier. The subsequent ringdown decay waveform is recorded and sent to a computer for analysis. The intensity of light transmitting through the exit mirror is linearly proportional to the intensity still trapped inside the cavity, therefore the intensity decay monitored at the photomultiplier follows the expression

$$I(t)=I_0e^{(-Ttc/2L)}, \tag{1}$$

where T is the transmission coefficient of the two mirror cavity, L is the mirror spacing, and t is time. Measurement of the cavity "ringdown" time (t, wherein $I=I_0e^{-1}$) allows the "transmissivity" of (or absorption inside) the cavity to be determined. This cavity transmissivity represents the total losses experienced by the light pulse per pass, including mirror reflectivity, optical scattering, mirror coating absorption, and molecular absorption. A plot of cavity losses versus wavelength allows an absorption spectrum to be obtained for species placed in the cavity. Accurate relative absorption intensities for molecular transitions (in the limit of weak absorption) are readily determined by comparing cavity losses with and without the sample present. Typically, 16 laser shots are averaged per wavelength step in order to reduce the noise introduced by fluctuations in the pulsed molecular beam. All of the data presented in this report were calibrated using the known vibronic spectra of the aluminum dimer, measured while vaporizing an aluminum rod in a He expansion.[20]

B. Gold silicide generation and TOFMS

In the present study, gold silicides are produced in the laser vaporization plasma reactor in the same fashion that copper and silver silicides were produced (see Refs. 18 and 19). A gas pulse consisting of a mixture of $<1\%$ silane in He is passed over a 0.5 in. Al rod wound with 0.020 in. thick gold wire which is simultaneously irradiated with a focused 248 nm excimer laser. The Au–Si plasma clusters in the throat of the nozzle and expands into the vacuum chamber, producing internally cold gold silicides. Optimum silicide production is achieved with ~100 mJ of laser light and ~80 psi of the gas mixture. Photoionization of neutral clusters is achieved with either the unfocused third harmonic (355 nm) of a Nd:YAG laser, or a KrF (248 nm) excimer laser. Resultant time-of-flight mass spectra are shown in Fig. 2. Of particular interest in this spectrum (2a) is the large relative intensity of the AuSi diatom peak, which is most likely due to a resonance enhancement with the 355 nm light. Comparison with the 248 nm data (2b) supports this conclusion. An optically accessible state near either the first or second steps (or both) of the multiphoton ionization process would explain this signal enhancement. In fact, the $D-X$ (0-1) vibronic transition lies less than 10 cm^{-1} to the red of 355 nm, and could explain these results if this transition was sufficiently power broadened. Nevertheless, it appears that gold silicides of various stoichiometries are readily formed in our molecular beam plasma reactor source. The ringing evident in some of the stronger peaks is a result of overdriving the preamplifier in the digital oscilloscope, and only occurs when the higher sensitivity settings of the scope are used (e.g., 1 mV/div.). There are currently no other Au–Si cluster mass spectrometric studies to compare with our data, and ambiguities

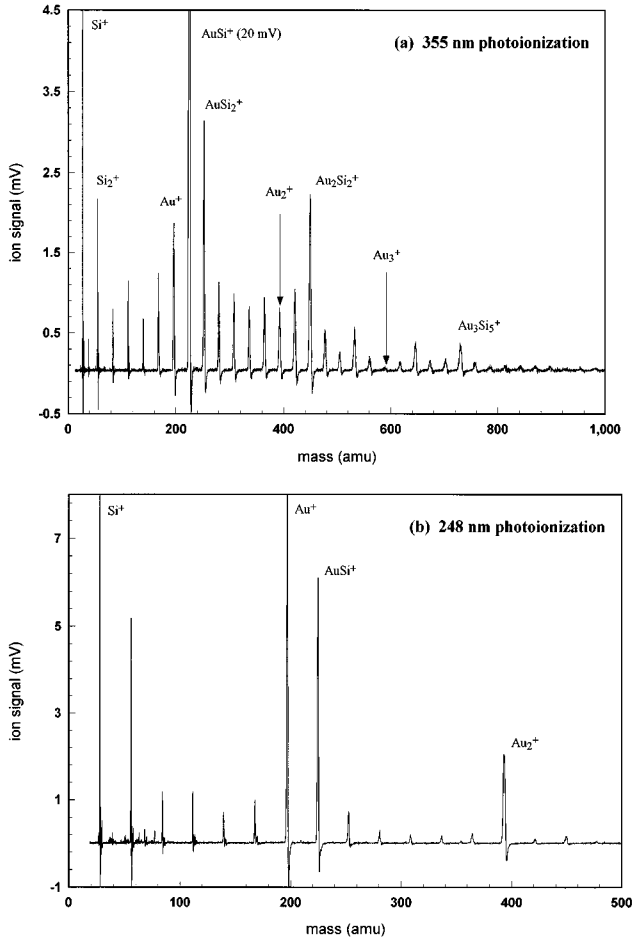

FIG. 2. (a) Time-of-flight mass spectrum of gold, silicon, and gold silicide clusters taken with 355 nm ionization. (b) Same conditions as above except with 248 nm ionization. Each scan is averaged over 5000 laser shots.

associated with multiphoton ionization prevent the further interpretation of our mass spectra at this time.

III. ANALYSIS AND DISCUSSION

Absorption spectra of gold silicides were obtained in the same wavelength region (340–400 nm) where spectra of copper and silver silicides were measured.[18,19] In total, 15 vibronic bands have been measured which are present only under source conditions which produce gold silicides. The first system consists of three bands in the 390 nm region which do not follow a regular vibrational progression. Of these three bands, one shows rotational structure, but it is severely congested and has not yet been assigned, and the other two are too weak to be analyzed. This band system will therefore not be discussed here. A second system, measured around 350 nm, possesses regular vibrational progressions and well resolved rotational features. These bands have been rovibronically analyzed to yield spectroscopic constants for the ground and excited states, and are assigned to the AuSi diatom.

A. Vibrational analysis

Of the 12 bands measured in the 340–365 nm region, 8 have been assigned to transitions between ground vibronic

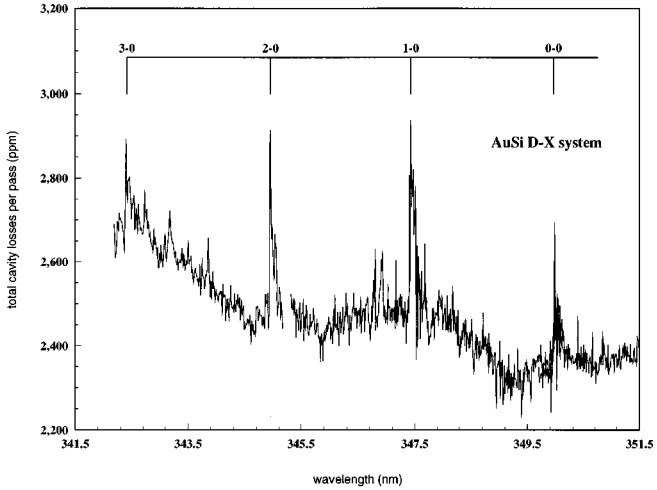

FIG. 3. Partial spectrum of the $D-X$ system of AuSi observed at low (0.3 cm^{-1}) resolution. This spectrum is a composite of 4 separate scans wherein 16 laser shots per wavelength point are averaged.

levels and a single upper electronic state of AuSi, as shown in the low resolution scan of Fig. 3. The D label has been chosen for this upper state for the following reasons: the A state had been assigned to the two band systems previously mentioned. Since no evidence of common upper states was obtained in the previous work, we reserve the B state as possibly belonging to the 750 nm system which was assigned as $A\ ^2\Sigma - X\ ^2\Pi_{1/2}$. Finally, we reserve the C state designation as possibly belonging to the three unassigned bands in the 390 nm region mentioned above.

The bandhead positions (listed in Table I) were fit using the standard expression,

$$\nu = T_e + \omega'_\epsilon(v'+1/2) - \omega_\epsilon\chi'_\epsilon(v'+1/2)^2 - \omega''_\epsilon(v''+1/2) + \omega_\epsilon\chi''_\epsilon(v''+1/2)^2. \quad (2)$$

For the upper (D) state, the vibronic progression was easily identified, and should result in accurate constants for that state. Transitions originating from higher vibrational levels of the ground electronic state, on the other hand, were much less intense (and intermittent) and therefore the constants associated with the ground electronic state are expected to be

TABLE I. Bandhead positions for the vibronic bands of the AuSi $D-X$ system, observed in the 350 nm region.

$D-X$ ($\nu'-\nu''$)	Frequency (cm^{-1})
0-2	27 726.6
0-1	28 105.9
1-1	28 316
3-2	28 349
0-0	28 496.4
1-0	28 705.4
2-0	28 912.8
3-0	29 119.0
unassigned	28 496.7
	28 707
	28 915.5
	29 128.1

TABLE II. Molecular constants for the $D-X$ system of AuSi.

	X	D
T_e	0	28 590(1)
B_ν	0.1350(1) (ν=0)	0.1161(1) (ν=2)
r_ν, Å	2.257(1)	2.434 (1)
ω_ϵ	400(2)	210.34 (21)
$\omega_\epsilon\chi_\epsilon$	5.0(8)	0.70 (5)
D_e ($\times 10^7$)	0.61[a]	1.4[a]
D_e (eV)	3.3[b]	1.96

[a]Estimated using Eq. (13).
[b]Thermochemical value.

TABLE III. Rotational constants and corresponding bond lengths obtained by incrementally shifting the rotational assignment. Under no circumstance could the rotational assignment of Ref. 9 be obtained.

Line, assignment	B''_ν (cm^{-1})$\rightarrow r''_\nu$ (Å)		B'_ν (cm^{-1})$\rightarrow r'_\nu$ (Å)	
28 910.736, $P(2)$	.173	1.98	.154	2.12
10.736, $P(3)$	.154	2.12	.135	2.26
10.736, $P(4)$[a]	.135	2.26	.116	2.44
10.736, $P(5)$	.116	2.43	.097	2.67
10.736, $P(6)$	.098	2.65	.079	2.95

[a]Indicates final chosen assignment.

less reliable. Furthermore, the ground state vibrational constants obtained from the given assignment suggest that the lower state is perturbed. For this reason, when fitting to Eq. (2), bands originating from the $v''=0$ level were weighted more heavily ($\sigma = 0.1$ cm^{-1}) than the hot bands ($\sigma = 1.0$ cm^{-1}). The results of the vibrational analysis based on the given assignment are presented in Table II. Unfortunately, gold does not possess multiple naturally abundant isotopes, which would permit a check of this vibronic assignment. However, the four weak hot bands in our spectra strongly support the given assignment. In addition to the assigned bands listed in Table I, there are 4 unassigned bands which are blue shifted with respect to the D state bands. Attempts to fit these bands to a vibrational progression resulted in a negative anharmonic constant. One possible explanation for these bands is presented in the discussion, following the results of a Franck–Condon analysis.

B. Rotational analysis

CRLAS rovibronic spectra of the (2-0) band are shown in Fig. 4, with the chosen rotational assignment as indicated. All of the bands of the $D-X$ system appear to lack Q-branches, indicating $\Delta\Lambda(\Omega)=0$ transitions. The (2-0) band has been rotationally fit as a $^2\Sigma-{}^2\Sigma$ band, using the same term value expressions for the two spin-rotation states as used for AgSi (Ref. 19) and CuSi.[18] Molecular orbital considerations which are in support of this assignment are presented in the discussion section. The rotational contours in Fig. 4 suggest a large increase in bond length in the upper electronic state, which is generally consistent with the observed large decrease in vibrational frequency. The (2-0) band was initially fit for a wide range of rotational assignments by incrementally shifting the rotational quantum numbers. This was done for two reasons; the first was to see if the lower state constants given by Houdart *et al.* could be reproduced with any assignment. The second reason was to test the measured band intensities using the associated bond lengths and vibrational frequencies in a Franck–Condon simulation. The results of several of these fits are outlined in Table III, which presents benchmark P-branch assignments for the associated fits. Additionally, the entire 2-0 system was simulated based on these possible assignments, in order to check the bandhead position, intensity, and line positions. If our bands in fact originate out of the ground state, then our studies indicate a possible misassignment in the work of Coquant and Houdart, since it is not possible for us to obtain a lower state rotational constant close to their 0.0617 cm^{-1} reported value. In fact, in order to achieve this B-value, the origin would have to sit at the bandhead, which is not consistent with the observed spectra. This result is not surprising, since the 3.3 Å bond length calculated from this rotational constant is much longer than expected based on comparison to the 2.23 Å and 2.41 Å bond lengths of CuSi and AgSi, respectively, or would be expected from a simple Pauling bonding model.[22]

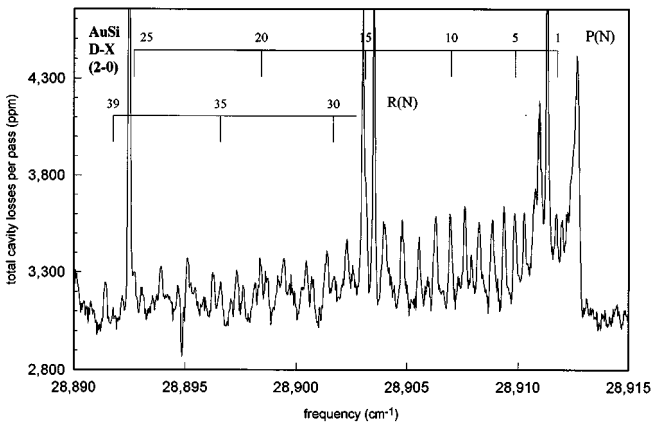

FIG. 4. The rotationally resolved 2-0 band of the AuSi $D-X$ system scanned at high (0.04 cm^{-1}) resolution. The rotational assignment is indicated in the figure. The additional large peaks evident in the scan are due to AuH.

The final results of the rotational analysis are indicated in Fig. 4, with the fitted rotational line positions and residuals listed in Table IV. Centrifugal distortion constants were not included in the rotational fits, since attempts to include them lead to either negative values or values with unacceptably large uncertainties. The distortion constants D_e listed in the table were therefore calculated using the standard relation

$$D_e = 4B_e^3/\omega_e^2, \tag{3}$$

IV. DISCUSSION

Molecular constants derived from the vibrational and rotational analysis are presented in Table II. The upper state well depth listed in the table has been calculated assuming a Morse potential with the estimation $D^e=\omega_e^2/4\omega_\epsilon\chi_\epsilon$. The vibrational constants obtained from measurements in this study are in general agreement with the ground state frequencies

TABLE IV. Measured rotational positions with assignments and residuals of the fit.

Assignment	Frequency (cm^{-1})
$R(11)$	28 912.302(−39)
$R(29)$	28 902.567(−13)
$R(31)$	28 900.756 (−9)
$R(32)$	28 899.805 (35)
$R(33)$	898.730(−26)
$R(34)$	897.687(−18)
$R(35)$	896.643 (28)
$P(7)$	909.384 (20)
$P(8)$	908.862 (32)
$P(9)$	908.278 (20)
$P(10)$	907.634(−14)
$P(11)$	906.988(−13)
$P(12)$	906.312 (−3)
$P(13)$	905.576(−16)
$P(14)$	904.839 (8)
$P(15)$	904.041 (8)
$P(17)$	902.321 (1)
$P(18)$	901.370(−10)
$P(19)$	900.480 (20)
$P(20)$	899.467 (−6)
$P(21)$	898.454 (7)
$P(22)$	897.380 (−4)
$P(23)$	896.306 (22)
$P(24)$	895.140 (−5)
$P(25)$	893.943(−26)
$P(26)$	892.747 (−8)

obtained from the low resolution work of Houdart and Schamps (400 cm^{-1} vs 391 cm^{-1}), although our anharmonicity is substantially larger (5.0 cm^{-1} vs 1.3 cm^{-1}). Two possibilities could explain this large anharmonicity; one is that the ground state is perturbed by another low lying electronic state, causing a distortion in the lower region of the well. The other possibility is that we have misassigned the (0,2) and (3,2) transitions. These transitions are reproducible yet very weak in our scans, and only the bandheads are observable. Nevertheless, this assignment is strongly supported by the fact that the spacing between these two bands matches the spacing between the (0,0) and (3,0) bands to within our frequency accuracy (<0.5 cm^{-1}). Without more information, however, this issue remains unresolved. For either of the above situations, a Morse potential estimate of the ground state well depth is not expected to be accurate. This calculation is omitted from our results for this reason. The large decrease ($\sim$50%) in vibrational frequency upon excitation into the upper electronic state is in qualitative agreement with the constants obtained from the rotational analysis.

The molecular orbital description of AuSi is essentially the same as that for CuSi and AgSi (Refs. 18 and 19). The ground state term symbols for Au and Si are ^2S and ^3P, respectively. If AuSi forms from ground state atoms, the possible molecular states are of $^2\Sigma$, $^2\Pi$, $^4\Sigma$, and $^4\Pi$ symmetry. These are the most likely candidates for the molecular ground state, since both Au and Si are known to readily form molecular bonds in their ground atomic states (e.g., Au_2, Si_2, AuAg, etc.). The silicon $3s^23p^2$ electronic configuration also gives rise to higher energy ^1D and ^1S states. Combining ^2S Au with ^1D Si yields $^2\Sigma$, $^2\Pi$, and $^2\Delta$ states, while the addition of ^1D and ^1S terms results in a single $^2\Sigma$ state. Other ground states are also possible if the molecule does not possess any of the above considered asymptotes. The apparent lack of Q-branches in our spectra is consistent with our $^2\Sigma$–$^2\Sigma$ assignment, but is also consistent with a $^4\Sigma$–$^4\Sigma$ assignment, in the case where the spin–spin splitting is not resolved. The lack of any resolvable splitting in the rotational features in our data, although inconclusive, is consistent with the present assignment.

As previously mentioned, the ground state had been assigned as a $^2\Pi$ state based on the presence of Q-branch heads in the previous low resolution work, and on the rotational assignment of Q-branches in the work of Coquant *et al.* (Ref. 9). It is possible that the observed band systems were actually due to $^2\Pi$–$^2\Sigma$ transitions, since the only way to distinguish between this assignment and the former (Σ–Π) would be by resolving the origin gap, which would be unlikely if there were both red degraded R and Q-branches. Both prior fluorescence studies employed high temperature oven sources. Therefore, another possibility is that these emission bands did not terminate in the ground state. To explore this possibility, we searched for the 1-0 band of the reported 710 nm band system, but did not observe any spectral features. Due to a lack of high reflectance mirror coverage (for $\lambda>720$ nm), we were not able to scan for the associated 0-0 band, which was reported as being more intense. Therefore, the fact that we have not seen this band system is not conclusive. Regardless, the above reversed state symmetry hypothesis is most consistent with our results, due to the agreement between the ground state vibrational frequency determined from our work and from the previous study.

Using the vibrational constants given in Table II, several Franck–Condon analyses[23] have been performed, using the bond lengths associated with the different rotational assignments of Table III. The FC factors associated with the different pairs of rotational constants did not appreciably change for the different assignments. This is expected, since the change in the difference between the bond lengths from one rotational fit to the next is small. Qualitatively, the measured band intensities are different from those calculated for all of the simulations. For example, the FC simulation for the chosen assignment predicts that the 3-0 band will be the strongest, while the experimental data show the 2-0 as the strongest. The trend observed is that the intensities of the upper state progression fall off much more rapidly than expected, which could possibly be explained by an upper state perturbation. The unassigned bands in Table I which are all shifted slightly to the blue of the fundamental progression provide a basis for this suggestion. Attempts to fit all 4 of these bands to a separate vibronic progression produced a negative anharmonicity. Additionally, hot band progressions of the D–X system would get closer to the fundamental bandheads with increasing vibrational quanta in the D state, in contrast to the observed increased spacing. One possible explanation for these additional bands is that a strong mixing is occurring between the D state and another electronic state, with an associated increased mixing with increasing D state vibrational quantum number. This would also be consistent with the increasing unassigned band intensity with decreasing

$D-X$ band intensity. In further support of this suggestion are the relative intensities of bands which terminate on common $\nu'=0$ states of the D state. These band intensities are closer to those predicted in the FC analysis, suggesting that states terminating on higher vibrational levels of the upper electronic state are more strongly perturbed. *Ab initio* calculations of the excited states in this region would be of great assistance in the resolution of this issue. In light of the above considerations, the vibronic analysis of all of the observed features is not yet definitive, although the $D-X$ upper state progression is confidently assigned at this time. The constants obtained in this work are also found to be consistent with the constants of the other coinage metal silicides, and indicate specific bonding trends.

V. COMPARISON WITH AgSi AND CuSi

From the CRLAS data presented in this paper, regular bonding trends emerge for the three coinage metal silicide diatoms. All three of the coinage metal silicides possess $^2\Sigma$ ground states (see also Refs. 18 and 19). This fact points to important possible bonding subtleties between silicon and metal atoms. Extension of the simple molecular orbital concepts presented for AgSi and CuSi to include AuSi explain the stronger bonding character of AuSi. The difference in electronegativity between Au and Si is $\sim$0.6, which leads to an expected ionic bonding contribution of $\sim$10%. This increased bond strength is evidenced by the increased force constant of AuSi derived from the ground state vibrational frequency. Similarly, the 2.26 Å bond length of AuSi is slightly less than the sum of the two atomic covalent radii, as expected, and is appropriately less than that of AgSi. These points are also in agreement with the measured ground state dissociation energy of 3.3 eV obtained by Gingerich *et al.*, which is substantially larger than the corresponding dissociation energies of both CuSi (2.25 eV) (Ref. 24) and AgSi (1.88 eV).[18] The ground state properties derived from the data and discussions presented for the three coinage metal silicides are important for understanding the detailed bonding of metal silicide species. Extension of these studies to include larger clusters as well as transition metals from other columns of the Periodic Table would provide an interesting test of the conclusions drawn from this work. These studies are currently underway in our laboratory.

ACKNOWLEDGMENTS

This research was supported by the Air Force Office of Scientific Research under Grant No. F49620-93-1-0278. J.J.S. thanks I.B.M. for a predoctoral fellowship during part of this research.

[1] O. Bisi, C. Calandra, L. Braicovich, and I. Abbati, J. Phys. C **15**, 4707 (1982).
[2] N. Toyama, J. Appl. Phys. **55**, 4398 (1984).
[3] N. G. Dhere and C. De A. Loural, Thin Solid Films **81**, 213 (1981).
[4] F. H. Baumann and W. Schroter, Phys. Rev. B **43**, 6510 (1991).
[5] A. Christou, Conference paper 5th spring meeting of AIME, p. 149, 1983 (unpublished).
[6] R. F. Barrow, W. J. M. Gissane, and D. N. Travis, Nature **201**, 603 (1964).
[7] K. A. Gingerich, J. Chem. Phys. **50**, 5426 (1969).
[8] R. Houdart and J. Schamps, J. Phys. B **6**, 2478 (1973).
[9] C. Coquant and R. Houdart, C. R. Acad. Sc. Paris **284**, 171 (1977).
[10] J. J. Scherer, J. B. Paul, A. O'Keefe, and R. J. Saykally, in *Advances in Metal and Semiconductor Clusters*, edited by M. A. Duncan (Jai, Greenwich, CT, in press), Vol. III.
[11] A. O'Keefe, and D. A. G. Deacon, Rev. Sci. Instrum. **59**, 2544 (1988); see also, A. J. Ramponi, Fred P. Milanovich, T. Kan, and D. Deacon, Appl. Op. **27**, 4606 (1988); J. M. Herbelin, J. A. McKay, M. A. Kwok, R. H. Ueunten, D. S. Urevig, D. J. Spencer, and D. J. Benard, *ibid*. **19**, 144 (1980); J. M. Herbelin and J. A. McKay, *ibid*. **20**, 3341 (1980); D. Z. Anderson, J. C. Frisch, and C. S. Masser, *ibid*. **23**, 1238 (1984).
[12] A. O'Keefe, J. J. Scherer, A. L. Cooksy, R. Sheeks, J. Heath, and R. J. Saykally, Chem. Phys. Lett. **172**, 214 (1990).
[13] D. Romanini and K. K. Lehmann, J. Chem. Phys. **99**, 6287 (1993).
[14] D. Romanini and K. K. Lehmann, J. Chem. Phys. **102**, 633 (1995).
[15] T. Yu and M. C. Lin, J. Am. Chem. Soc. **115**, 4371 (1993).
[16] G. Meijer, M. G. H. Boogaarts, R. T. Jongma, D. H. Parker, and A. M. Wodtke, Chem. Phys. Lett. **217**, 112 (1994).
[17] P. Zalicki, Y. Ma, R. N. Zare, E. H. Wahl, J. R. Dadamio, T. G. Owano, and C. H. Kruger, Chem. Phys. Lett. **234**, 269 (1995).
[18] J. J. Scherer, J. B. Paul, C. P. Collier, and R. J. Saykally, J. Chem. Phys. **102**, 5190 (1995).
[19] J. J. Scherer, J. B. Paul, C. P. Collier, and R. J. Saykally, J. Chem. Phys. **103**, 113 (1995).
[20] Z. Fu, G. W. Lemire, G. A. Bishea, and M. D. Morse, J. Phys. Chem. **93**, 8420 (1990).
[21] G. Herzberg, *Spectra of Diatomic Molecules* (Van Nostrand, New York, 1953), Chap. VI.
[22] L. Pauling, J. Am. Chem. Soc. **69**, 542 (1947).
[23] Program generously supplied by Dr. Don Arnold. Current address: University of Southern California, Department of Chemistry, Los Angeles, California 90089.
[24] G Riekert, P Lamparter, and S. Steeb, Z. Metallkd. **72**, 765 (1981).